JOURNAL OF MATERIALS SCIENCE 28 (1993) 4023–4027

In situ fracture monitoring of plasma-sprayed $MoSi_2$–Ta composites

J. D. RIGNEY*, R. G. CASTRO‡, J. J. LEWANDOWSKI*
*Case Western Reserve University, Cleveland, OH 44106, USA
‡Los Alamos National Laboratory, Los Alamos, NM 87545, USA

Initial work has shown that the ambient toughness of brittle silicide intermetallics such as $MoSi_2$ have been toughened by incorporating irregular pancake-shaped Ta phases via deposition of powders by plasma-spray processing techniques. The mechanisms of toughness enhancement were observed *in situ* by conducting fracture toughness tests in an instrumented loading stage situated in a scanning electron microscope. It was observed that increases in toughness were obtained via ductile-phase toughening and the development of bridged-zones. The initiation and peak toughness of the composites varied with testing orientation, with the highest values measured when the crack plane intersected the Ta particles perpendicular to their edge. The shape of the resistance curve, however, was independent of Ta orientation.

1. Introduction

Silicides and silicide-based composites provide a number of attractive features for potential high-temperature service [1–5]. One system of recent interest is based on the Mo–Si system [1–5], where $MoSi_2$ has a melting point of 2303 K and is expected to possess high-temperature strength, stiffness and creep resistance [4–6]. However, a low value of fracture toughness [7] ($\sim 5\,MPa\,m^{1/2}$) and inadequate ambient ductility [7] limit its application. Recent work [7, 8] has indicated that grain-boundary SiO_2 is detrimental to mechanical properties over a range of temperatures, while alloying with carbon has shown to provide increased toughness at both intermediate and high temperatures via the removal of SiO_2 and production of SiC [7, 8]. The present work investigates the feasibility of toughening these materials by ductile-phase toughening through a plasma spray technique [9]. The technique has been used to deposit Ta particles while depositing prealloyed $MoSi_2$ powders.

A variety of brittle-matrix systems have realized toughening as a result of dispersed ductile phases, such as Nb_5Si_3–Nb [1–4], NiAl–Mo [10], Al_2O_3–Al [11, 12], SiC–Al [13–15], TiAl–(Nb or NbTi) [16, 17], WC–Co [18, 19] and $MoSi_2$–Nb [20] in addition to model systems such as glass–Pb [21], glass–(Al or Ni) [22] and epoxy–rubber [23]. As described in several analyses [20–25], one proposed mechanism of ductile-phase toughening is ductile bridging of intact ligaments behind the crack tip along the fracture plane. The degree of toughening in these analyses is proposed to depend primarily on the stress–strain behaviour (yield stress and degree of plastic stretching) of the ductile ligament while constrained by the elastic matrix. The extent of interfacial debonding controls the constraint and stress–strain behaviour of the ligament, thereby affecting the magnitude of toughening. The toughening is also proposed to be related to the area fraction and radius of the ligaments intercepted in the fracture plane [20–25]. Recent work [1, 4, 26] has begun to measure the extent of bridging *in situ* in bulk composite specimens and its effects on resultant resistance (R-curve) behaviour. The present work was undertaken to monitor the interaction of matrix cracks with Ta dispersions, the mechanical response of the particles, the development of bridged-zones and the resultant effect on R-curve behaviour in $MoSi_2$ toughened with 20 vol % Ta. The intent was also to observe the orientation dependence of the resistance to crack propagation due to the aspect ratio of the metal inclusions in the brittle matrix.

2. Experimental procedure

The materials investigated were produced at Los Alamos National Laboratory by co-deposition of $MoSi_2$ and tantalum using low-pressure plasma spraying. The source powders used for the plasma-spray process were sieved to $-200+325$ mesh and had an average particle size of 60 μm. The operating pressure for depositing these powders was held at approximately 300 torr to take advantage of the controlled atmosphere and higher substrate temperature (~ 1173 K) needed in order to produce free-standing spray-form deposits of the $MoSi_2$–Ta composite. A spray-form deposit approximately 60 mm in length

0022–2461

$\times$ 20 mm in width $\times$ 6 mm in height (in the sprayed direction) was produced for the current experiments. Experimental details containing the optimized spray parameters used in co-depositing these materials which yielded spray-forms loaded to $\sim$20 vol % Ta dispersed in the $MoSi_2$ matrix can be found elsewhere [9].

Notched three-point bend bars with typical height (W) by thickness (B) dimensions of 6 mm $\times$ 2 mm were electro-discharge machined (EDM) from the spray deposit. Notches were either put in place by EDM (125 μm notch root radius) to a partial depth of $a/W \simeq 0.3$ and then finished to $a/W \simeq 0.45$–0.55 by a high-speed wire saw (30–40 μm notch root radius). Most samples/notches were oriented so that cracks would propagate and intersect Ta particles face-on the splats (i.e. crack plane in the direction of and containing the spraying direction) while others were oriented to intersect Ta particles edge-on (crack plane perpendicular and containing the spraying direction). The samples were loaded in order to test the samples with height (W) by span (S) ratios of $S/W \simeq 4/1$ in accordance with standard fracture toughness testing procedures [27]. One or both sides of the samples were polished to a 0.05 μm Al_2O_3 finish to facilitate fracture monitoring via scanning electron microscopy (SEM) techniques.

The specimens were tested under displacement control at $\sim$ 1 μm s^{-1} on a Jeol 840A SEM equipped with an Oxford Instruments deformation stage. The deformation stage may be operated in tension, compression or bending and provides a range of crosshead displacement rates ($\sim$ 1–4 μm s^{-1}) in addition to real-time monitoring of load, displacement and crack length. Strip-chart recorders and computer-aided data acquisition were used to record load versus time traces for the various tests that were conducted, and were later converted to load–load point displacement traces. SEM photographs and videotapes of crack growth using secondary electron emission were utilized to monitor and measure instantaneous crack growth. The SEM electron beam in the experiments was oriented perpendicular to the sample surface. The loads (P_Q) at which initial and subsequent cracking events were observed were used in the following equation [27] to determine the initiation toughness of the sample as well as R-curve behaviour:

$$K_Q = \left(\frac{P_Q S}{B W^{3/2}}\right) f(a/W)$$

In situ monitoring of the test provided information on the instantaneous crack length and load, enabling the construction of K versus Δa curves. Post-failure analysis consisted of SEM examination of the fracture surfaces to observe the fracture behaviour of the Ta. Fractured samples from both face-on and edge-on orientations were mounted and polished into the mid-plane of the sample ($\sim$ 1 mm) to reveal the behaviour of the $MoSi_2$–Ta interfaces in the region of the resistance curve.

3. Results and discussion

Fig. 1 shows the typical appearance of the $MoSi_2$–Ta composite in the three orthogonal views, along with the orientation of the notched bend specimens with respect to the microstructure (i.e. face-on or edge-on the Ta particles). The Ta particles, showing the lightest contrast in Fig. 1, occupy approximately 20 % by volume. The average aspect ratio of the irregular pancake-shaped Ta particles is $\sim$ 5:1 with typical dimensions of 50–100 μm $\times$ 4–8 μm. Phases with contrast between that of the dark $MoSi_2$ matrix and that

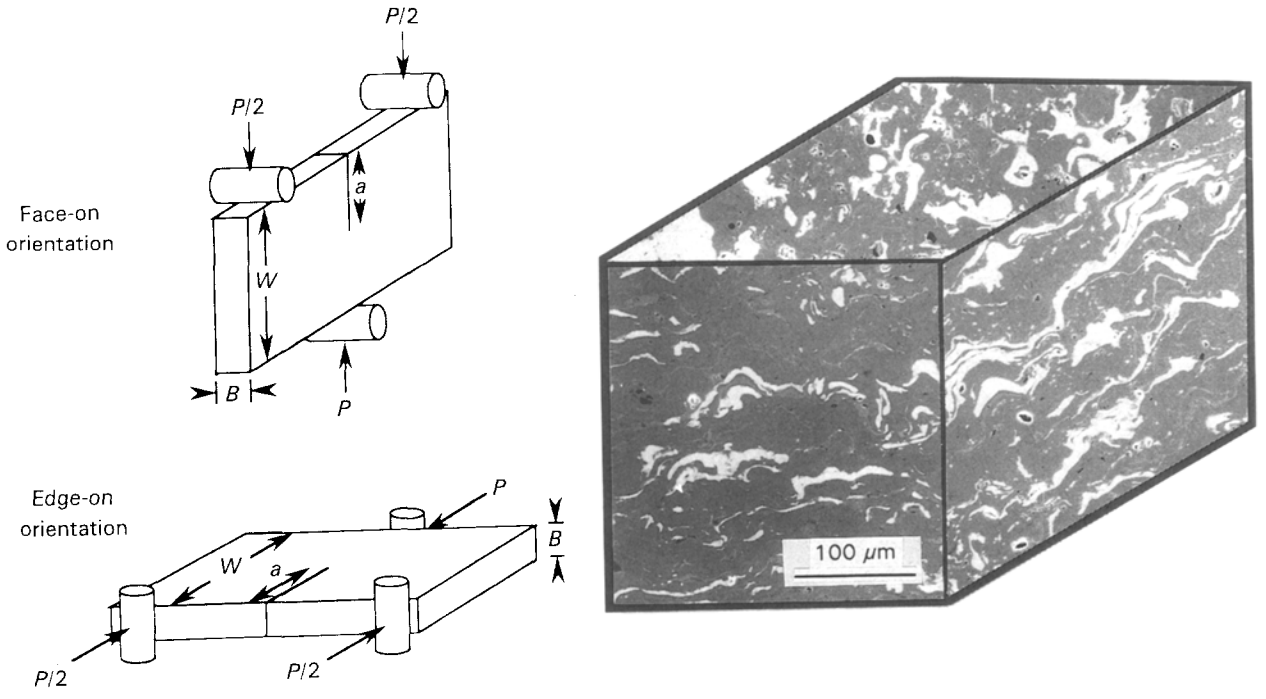

Figure 1 Microstructure of $MoSi_2$–Ta composite with orientation of mechanical testing shown. Aspect ratio of the particles is $\sim$ 5:1.

of the reinforcement are areas lean in Si. Density of the structure was approximately 97 % theoretical. Oxygen contents in the as-sprayed materials were of the order of 300 p.p.m.

Fig. 2 shows load–load point displacement traces obtained during *in situ* fracture toughness testing of the three-point bend specimens. The differences in the two traces (open versus filled circles) are typical of those found for the two test orientations with respect to the microstructure (as shown in Fig. 1). The load drops shown are due to manual decreases in load. At the onset of observed crack extension (from the secondary electron function in the SEM), the crosshead motion was reversed to enable detailed examination of the formation of any bridged-zones. The specimens were subsequently reloaded at a 1 $\mu m\,s^{-1}$ displacement rate.

Fig. 3 summarizes the K versus Δa curves obtained for the face-on (five samples) and edge-on (one sample) oriented samples. The figure indicates that in both orientations steeply-rising R-curves are obtained, where the initiation toughnesses are $\sim 3\ MPa\,m^{1/2}$ for the face-on and $5\ MPa\,m^{1/2}$ for the edge-on orientations, increasing to 8 and $9\ MPa\,m^{1/2}$, respectively, with 700 μm of crack extension. The results suggest that the edge-on oriented samples are tougher in that their initiation toughness is higher and they rise to a higher (measured) peak toughness than the face-on oriented samples. However, the rise in the resistance to fracture (slope of the K–Δa curve) is essentially independent of orientation. Bridged-zones were of the order of 400 μm for both materials.

Fig. 4 shows two SEM photographs of a crack progressing in a face-on oriented sample. In Fig. 4a a crack has grown in the $MoSi_2$ matrix and has intercepted several (i.e. four) Ta particles in the micrograph, labelled A to D. Near the notch the crack has fractured particle A without measurable plasticity, avoided particle B and then intercepted particles C and D without fracture. Upon further loading to higher stress intensities (Fig. 4b), particle C deformed with observable plasticity and particle D fractured. These events, both deflection off and crack bridging by Ta particles and eventual ductile and brittle fracture of the Ta, contribute to the R-curve behaviour observed and quantified in Fig. 3. Further loading of the sample resulted in the fracture of the intact ligament and little interfacial debonding was noted. Similar fracture events, i.e. crack deflection and bridging, were observed for the samples oriented in the edge-on configuration.

Consistent with the *in situ* observations, the fracture surface details near the notch also illustrate the ductile behaviour of the Ta, as shown in Fig. 5a. Fig. 5b is a matching back-scattered electron image of the fracture

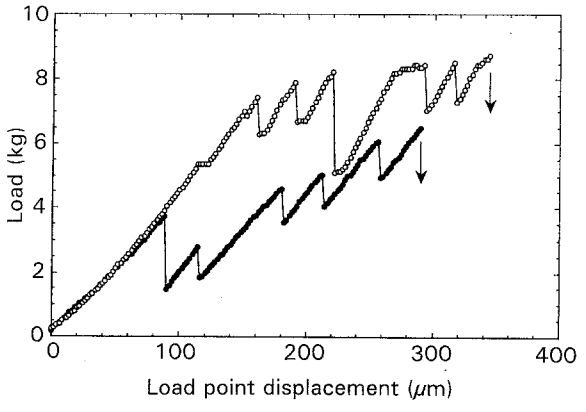

Figure 2 Load–load point displacement curves acquired from the *in situ* three-point bend tests on (●) face-on and (○) edge-on oriented $MoSi_2$–Ta samples.

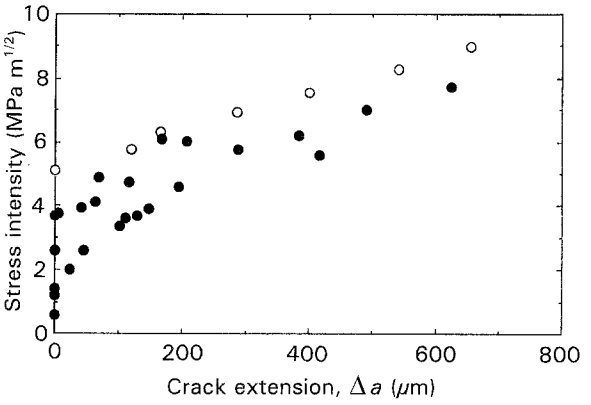

Figure 3 K versus Δa plot constructed from *in situ* fracture observations and Fig. 2: (●) face-on, (○) edge-on Ta particles

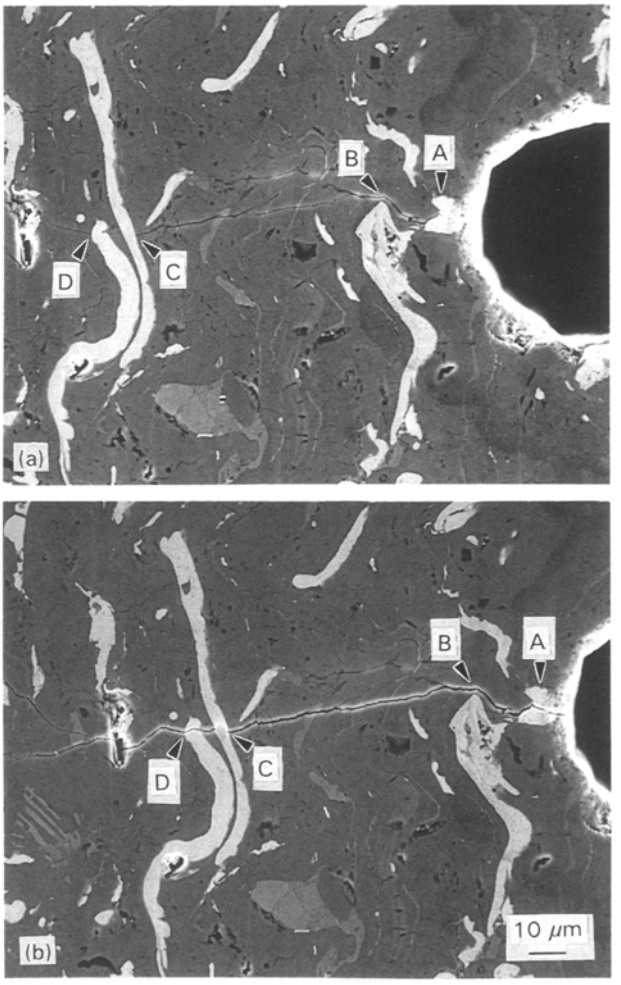

Figure 4 Crack propagation/bridging events observed during *in situ* testing of the face-on oriented samples. A crack progressing in the matrix has been influenced by particles A to D. (a) Fracture of A and avoidance of B and bridging of C and D observed. (b) Load increase has caused ductile behaviour of C but brittle fracture in ligament D.

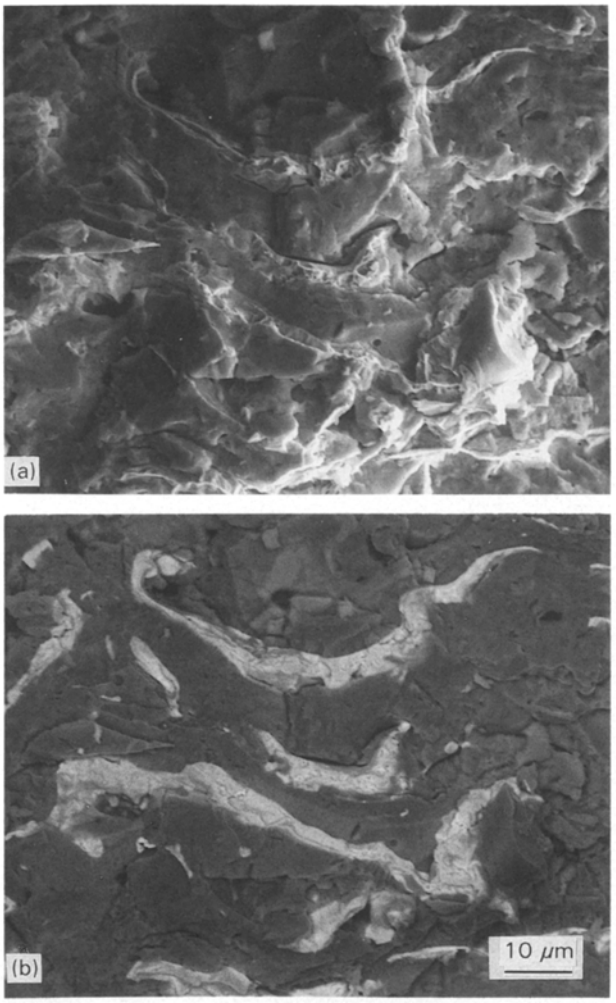

Figure 5 Ductile fracture of Ta particles on the fracture surface near the notch in the range of the resistance curve: (a) secondary electron image and (b) matching back-scattered electron image.

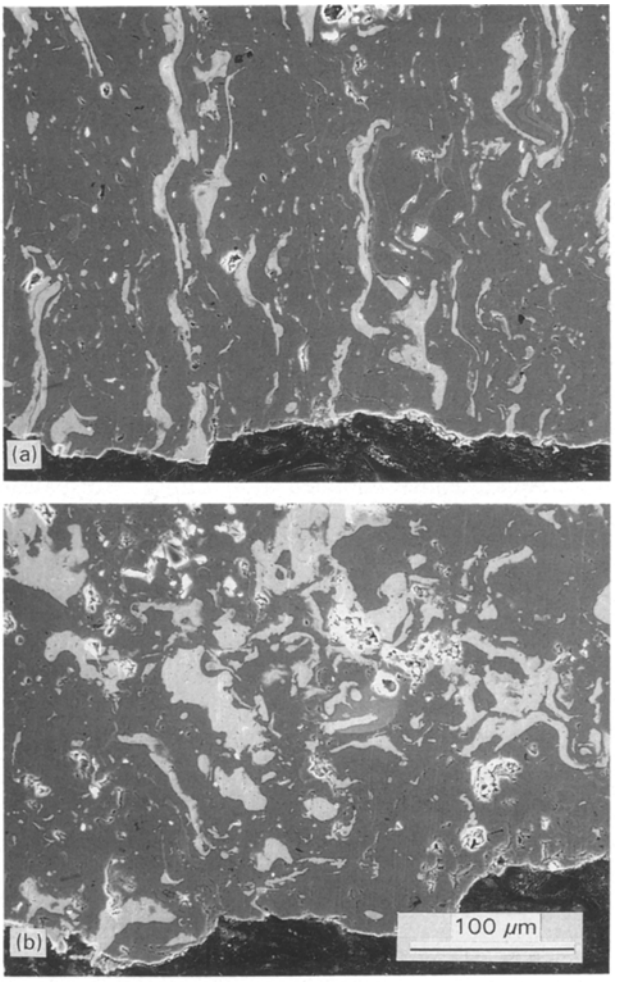

Figure 6 Polished cross-sections of both composite sample orientations showing little interfacial debonding behaviour: (a) face-on and (b) edge-on orientation.

surface highlighting the regions of Ta (lighter contrast). Cross-sections of the fracture surfaces (Fig. 6) from both sample types indicate that little debonding accompanies crack propagation along the sample mid-section.

According to the models of ductile-phase toughening, the mixed ductile and brittle fracture behaviour of the Ta and the evidence of little debonding, indicate that the maximum composite toughness may not have been achieved. The models indicate that some degree of interfacial debonding is necessary for highest peak toughness as the ductile phase deforms and fails in the bridged zone. The current results suggest that the Ta failed either in the linear-elastic portion of their stress–strain curves or without significant debonding. Work on steels [28, 29] and more recently on ductile-phase toughened Nb_5Si_3–Nb [30–32] has shown that the appearance of cleavage fracture, however, does not necessarily indicate low toughness. Research is continuing to change the properties of the Ta so that brittle fracture is avoided.

The initiation and peak toughnesses of the composites compare well with chevron-notched fracture toughness tests conducted on identically processed materials [9]. Molybdenum disilicide without reinforcement had toughness values of 4.97 ± 0.351 and $4.50 \pm 0.173\,MPa\,m^{1/2}$ in the edge-on and face-on orientation, respectively [9]. With additions of 20 vol% Ta to the $MoSi_2$ matrix, peak toughness values, which do not account for crack extension as measured in the current report, were 9.97 ± 0.25 and $8.0 \pm 0.30\,MPa\,m^{1/2}$, again in the edge-on and face-on orientations, respectively. The values measured currently were similar in relative magnitude, with the initiation and peak toughnesses both higher in the edge-on orientation. This is the expected trend since the initiation of cracks in the matrix is governed by the toughness of the matrix, while the peak toughness is governed by the interaction of matrix cracks with the Ta particles (i.e. deflection off or bridging by Ta).

Ductile-phase toughened γ-TiAl composites, processed by conventional powder processing and hot forging, have also been produced to have platelet-shaped reinforcements dispersed throughout the matrix [17]. The fracture and R-curve behaviour of materials containing either Ti6Al4V, Nb or NbTi have been investigated with respect to orientation. The fracture resistance was determined to be highly dependent on the deformation behaviour of the metal inclusion and the interfacial characteristics. Only in the case of the TiAl–Nb, in which significant debonding and ductile behaviour of Nb was observed, was an

orientation dependence on the fracture toughness observed. In this case, the edge-on oriented samples displayed lower initiation and peak toughness values than those in the face-on orientation. The higher values were proposed to result from the more tortuous fracture path in the face-on orientation. In the cases of TiNb- or Ti6Al4V-reinforced TiAl, the initiation and peak values were independent of orientation as was the resistance to fracture. However, the slopes of the K–Δa curves were similar with respect to the two orientations in each composite type, as was found in the current investigation.

4. Conclusions

1. The toughness and mechanisms of toughness enhancement in $MoSi_2$–Ta composites was evaluated using *in situ* fracture monitoring. Crack bridging of Ta particles was observed and R-curve behaviour was exhibited and quantified.

2. The orientation of fracture with respect to the microstructure affected the initiation and peak toughnesses of the samples tested. Samples oriented so that cracks intersected the Ta particles perpendicular to their edge exhibited higher initiation and peak toughnesses than those oriented perpendicular to their face.

3. Crack bridging by the Ta particles was observed to cause a significant rise in the crack resistance curve at small crack lengths. Both ductile and brittle behaviour of the Ta was observed during crack propagation.

4. Work is continuing to optimize the microstructures produced during plasma spraying and to increase the ductility of the Ta particles.

Acknowledgements

The work at CWRU was supported by AFOSR under contract no. 89-0508, with Dr Alan Rosenstein as contract monitor, with partial support by MTS Systems Corporation.

References

1. J. J. LEWANDOWSKI, D. M. DIMIDUK, W. KERR and M. G. MENDIRATTA, "High temperature/High Performance Composites", Materials Research Society Symposium Proceedings, Vol. 120, edited by F. D. Lembey, A. G. Evans, S. G. Fishman and J. R. Strife (Materials Research Society, Pittsburg, PA, 1988) p. 103.
2. M. G. MENDIRATTA and D. M. DIMIDUK, "High Temperature Ordered Intermetallic Alloys III", Materials Research Society Symposium Proceedings, Vol. 133. (Materials Research Society, Pittsburg, PA, 1989) p. 441.
3. R. M. NEKKANTI and D. M. DIMIDUK, "Intermetallic Matrix Composites", Materials Research Society Symposium Proceedings, Vol. 194, edited by D. L. Anton, P. L. Martin, D. B. Miracle and R. McMeeking (Materials Research Society, Pittsburg, PA, 1990) p. 175.
4. M. G. MENDIRATTA, J. J. LEWANDOWSKI and D. M. DIMIDUK, *Metall. Trans. A.* **22A** (1991) 1573.
5. R. L. FLEISHER, *J. Mater. Sci.* **22** (1987) 2281.
6. *Idem, J. Metals* **12** (1985).
7. S. A. MALOY, J. J. LEWANDOWSKI, A. H. HEUER and J. PETROVIC, *J. Amer. Ceram. Soc.* **74** (1991) 2704.
8. *Idem, Mater. Sci. Eng.* **A155** (1992) 159.
9. R. G. CASTRO, R. W. SMITH, A. D. ROLLETT and P. W. STANEK *Mater. Sci. Eng.* **A155** (1992) 101.
10. P. R. SUBRAMANIAN, M. G. MENDIRATTA, D. B. MIRACLE and D. M. DIMIDUK, "Intermetallic Matrix Composites", Materials Research Society Symposium Proceedings, Vol. 194, edited by D. L. Anton, P. L. Martin, D. B. Miracle and R. McMeeking (Materials Research Society, Pittsburg, PA, 1990) p. 147.
11. B. D. FLINN, M. RÜHLE and A. G. EVANS, *Acta Metall.* **37** (1989) 3001.
12. L. S. SIGL, P. A. MATAGA, B. J. DALGLEISH, R. M. McMEEKING and A. G. EVANS, *ibid.* **36** (1988) 945.
13. J. J. LEWANDOWSKI, C. LIU and W. H. HUNT *Jr, Mater. Sci. Eng.* **A107** (1989) 241.
14. M. MANOHARAN, L. ELLIS and J. J. LEWANDOWSKI, *Scripta Metall.* **24**, (1990) 1515.
15. L. ELLIS and J. J. LEWANDOWSKI, *J. Mater. Sci. Lett.* **10** (1991) 461.
16. H. C. CAO, B. J. DALGLEISH, H. E. DÈVE, C. K. ELLIOT, A. G. EVANS, R. MEHRABIAN and G. R. ODETTE, *Acta Metall* **37** (1989) 2969.
17. C. K. ELLIOT, G. R. ODETTE, G. E. LUCAS and J. W. SHECKHERD, "High Temperature/High Performance Composites", Materials Research Symposium Proceedings, Vol. 120, edited by F. D. Lemkey, A. G. Evans, S. G. Fishman and J. R. Strife. (Materials Research Society, Pittsburg, PA, 1988) p. 95.
18. V. D. KRSTIC and M. KOMAC, *Phil. Mag. A* **51** (1985) 191.
19. L. S. SIGL and H. E. EXNER, *Metall. Trans. A* **18A** (1987) 1299.
20. T. C. LIU, A. G. EVANS, R. J. HECHT and R. MEHRABIAN, *Acta Metall.* **39** (1991) 1853.
21. M. F. ASHBY, F. J. BLUNT and M. BANNISTER, *ibid.* **37** (1989) 1847.
22. V. KRSTIC and P. S. NICHOLSON, *J. Amer. Ceram. Soc.* **64** (1981) 499.
23. S. KUNZ-DOUGLASS, P. W. R. BEAUMONT and M. F. ASHBY, *J. Mater. Sci.* **15** (1980) 1109.
24. B. BUDIANSKI, J. C. AMAZIGO and A. G. EVANS, *J. Mech. Phys. Solids* **36** (1988) 167.
25. P. A. MATAGA, *Acta Metall.* **37** (1989) 3349.
26. J. D. RIGNEY and J. J. LEWANDOWSKI, Ceramic transactions, Vol. 19, "Advanced Composite Materials", edited by M. D. Sacks. (American Ceramic Society, Westerville, OH, 1991) p. 519.
27. "Standard Test Method for Plane Strain Fracture Toughness of Metallic Materials", ASTM Standard E399-83, in "Annual Book of ASTM standards", Vol. 03.01(ASTM, Philadelphia, PA, 1988) p. 480.
28. R. O. RITCHIE, J. F. KNOTT and J. R. RICE, *J. Mech. Phys. Solids* **21** (1973) 395.
29. J. J. LEWANDOWSKI and A. W. THOMPSON, *Metall. Trans. A* **17A**, (1986) 1769.
30. J. D. RIGNEY, unpublished research (1991).
31. J. KAJUCH, J. D. RIGNEY and J. J. LEWANDOWSKI, *Mater. Sci. Eng.* **A155** (1992) 59.
32. J. D. RIGNEY, P. M. SINGH and J. J. LEWANDOWSKI, *J. Metals*, **8** (1992) 36.

Received 5 February
and accepted 8 December 1992